IRON-NICKEL NANOCRYSTALLINE PARTICLES – EFFECT OF PREPARATION OF PRECURSORS

[1]Eva ŠVÁBENSKÁ, [1,2]Pavla ROUPCOVÁ, [1,2]Lubomír HAVLÍČEK, [1]Oldřich SCHNEEWEISS

[1]Institute of Physics of Materials, AS CR, Brno, Czech Republic, EU, svabenska@ipm.cz

[2]CEITEC Brno University of Technology, Brno, Czech Republic, EU

https://doi.org/10.37904/nanocon.2024.5000

Abstract

Fe-Ni-based nanoparticles are promising materials for the production of high-performance permanent magnets. The research explores the preparation of Fe-Ni alloys using iron-nickel oxalate precursors, which were synthesized via the coprecipitation method and subsequently reduced in a hydrogen atmosphere. One of the aims of the work is to compare the effect of different methods of preparation of precursors on the particle size and composition of the resulting materials. Structural, magnetic, and morphological properties were analyzed using a combination of Mössbauer spectroscopy, X-ray powder diffraction (XRD), and scanning electron microscopy (SEM).

The relative proportions of iron and nickel content in the prepared oxalate precursors were approximately 50% by weight, according to EDS analysis. The precursor samples consisted of clusters of particles with undefined shapes, exhibiting a wide range of particle sizes. After annealing, multiple Fe-Ni phases were present in the sample. Structure investigation and magnetic measurements confirmed the formation of phases suitable for magnetic applications.

Keywords: Magnetic materials, thermal decomposition, Mössbauer spectroscopy, microscopy

1. INTRODUCTION

Magnetic Fe-Ni particles have a wide range of applications, including in the production of inductors, transformers, catalysts, and biomedical devices. [1, 2] The magnetic properties of these materials are heavily influenced by factors such as particle morphology, size, crystallinity, and purity, which are, in turn, dependent on the preparation method used. Various methods for synthesizing Fe-Ni particles have been explored, including mechanical milling [3, 4], coprecipitation [5, 6], chemical reduction [7], etc.

The present work is devoted to preparing Fe-Ni phases with suitable magnetic properties. The first part focuses on synthesizing and characterizing various oxalate precursors. The second part explores the formation of Fe-Ni alloys through thermal decomposition in a reducing atmosphere. The structural characteristics, particle sizes, and magnetic properties of the samples were comprehensively analyzed using a combination of Mössbauer spectroscopy (MS), X-ray diffraction (XRD), magnetization measurements (VSM), scanning electron microscopy (SEM), and energy-dispersive X-ray spectroscopy (EDS).

2. MATERIALS AND METHODS

2.1 Sample preparation

Mixed Fe-Ni oxalate dihydrate crystals were prepared by precipitation. The samples were prepared using 0.1 M solutions of $FeSO_4 \cdot 7H_2O$, $NiSO_4 \cdot 6H_2O$, $FeSO_4 \cdot (NH_4)_2SO_4 \cdot 6H_2O$, and $NiSO_4 \cdot (NH_4)_2SO_4 \cdot 6H_2O$, along with a 0.2 M solution of oxalic acid. Oxalate precursor samples were synthesized using the coprecipitation method, with slight variations in the preparation of each sample. For sample ES1, both sulfates were combined and

then added to the oxalic acid solution. In the case of sample ES2, sulfate solutions were alternately introduced into the oxalic acid. Sample ES3 followed the same sequential procedure as ES2, but the solutions were additionally treated with ultrasound. For samples ES4 and ES5, one of the sulfates was replaced with ammonium iron sulfate or ammonium nickel sulfate, respectively. The precipitate was isolated by filtration, washed several times with ethanol, and then dried

The oxalate precursor was characterized using microscopy, powder X-ray diffraction, and Mössbauer spectroscopy. After characterization, the samples were annealed in a laboratory furnace under a hydrogen atmosphere to study the effects of thermal treatment on the precursor materials.

2.3 Methods

The chemical composition of the samples was analyzed using a TESCAN LYRA 3XMU FEG/SEM scanning electron microscope equipped with an Oxford Instruments XMax80 detector for energy-dispersive X-ray spectroscopy. Secondary electron images and EDS spectra were obtained at accelerating voltages of 15 kV.

Phase composition studies were conducted using an Empyrean diffractometer (Panalytical) in Bragg-Brentano geometry with CoKα radiation (λ = 0.17902 nm) at room temperature. The resulting patterns were analyzed using the HighScore® software and the ICDD (PanAnalytical) database.

Transmission ^{57}Fe Mössbauer spectra of the studied samples were measured in the 5–293 K temperature range using a standard Mössbauer spectrometer in a constant acceleration mode with a ^{57}Co (Rh) radioactive source. The isomer shift values were referred to as the value of an α-Fe foil sample. The computer processing of the spectra was done using CONFIT program package [8].

Magnetic properties were measured with the EverCool II PPMS (Quantum Design) system using a VSM mode in the temperature range 4-300 K and with the magnetic field range of – 9T to + 9T. Additionally, a Vibrating Sample Magnetometer (VSM) equipped with a furnace capable of reaching up to 800°C and a magnetic field range of -1 T to +1 T was used for magnetic measurements.

3. RESULTS AND DISCUSSION

3.1 Characterization of precursor

The morphology of $Fe_{(1-x)}Ni_xC_2O_4$ particles was investigated using SEM. The samples were made up of a conglomerate of particles of different sizes. The particles displayed a wide range of shapes, from flakes to rectangular structures. According to EDS analysis, the relative proportion of iron and nickel in the prepared oxalate precursor was approximately 48% and 52% by weight, respectively. EDS maps show a homogeneous distribution of iron and nickel in the particles of individual samples.

The XRD patterns of the precursor were identified as Iron Oxalate Dihydrate ($FeC_2O_4 \cdot 2H_2O$). This result might be attributed to the substitution of ions or overlapping diffraction patterns, as iron and nickel oxalates have very similar peak positions, making it challenging to distinguish between them accurately. The XRD analysis estimated an average particle size of around 37 nm. The smallest particle size, approximately 27 nm, was observed in sample ES4, which was prepared using a combination of $FeSO_4 \cdot (NH_4)_2SO_4 \cdot 6H_2O$ and $NiSO_4 \cdot 6H_2O$.

The Mössbauer spectra of the precursors consist of two quadrupole doublets. The first doublet, with an isomer shift IS = 1.19±0.01 mm/s and quadrupole splitting QS_{pl} = of 1.70±0.02 mm/s, corresponds to Fe-Ni mixed-metal oxalates [9,10]. The second doublet, with IS = 1.29±0.02 mm/s and QS_{pl} = 2.3±0.04 mm/s, is associated with iron sulfate monohydrate. The observed quadrupole splitting values are lower than the reported 2.71 mm/s in the literature [11], which suggests that the increase in QS may be due to the presence of nickel ions in the sample. The phase composition, represented as the atomic fraction of Fe, ranges from 0.89 to 0.96 for the first

doublet (D1) and from 0.03 to 0.10 for the second doublet (D2). Detailed phase compositions for each sample are provided in **Table 1**.

Table 1 Hyperfine parameters resulting from the Mössbauer spectra analysis of oxalate precursors (IS - isomer shift, QS_{pl} - quadrupole splitting, A - phase content in atomic fraction of Fe).

Sample	D1			D2		
	IS (mm/s)	QS_{pl} (mm/s)	A	IS (mm/s)	QS_{pl} (mm/s)	A
ES1	1.18±0.01	1.71±0.01	0.96	1.29±0.01	2.39±0.04	0.04
ES2	1.19±0.01	1.71±0.01	0.95	1.29±0.01	2.35±0.01	0.05
ES3	1.18±0.01	1.70±0.01	0.93	1.29±0.01	2.34±0.06	0.07
ES4	1.19±0.01	1.72±0.01	0.93	1.29±0.01	2.35±0.05	0.07
ES5	1.19±0.01	1.70±0.01	0.89	1.29±0.01	2.25±0.10	0.10

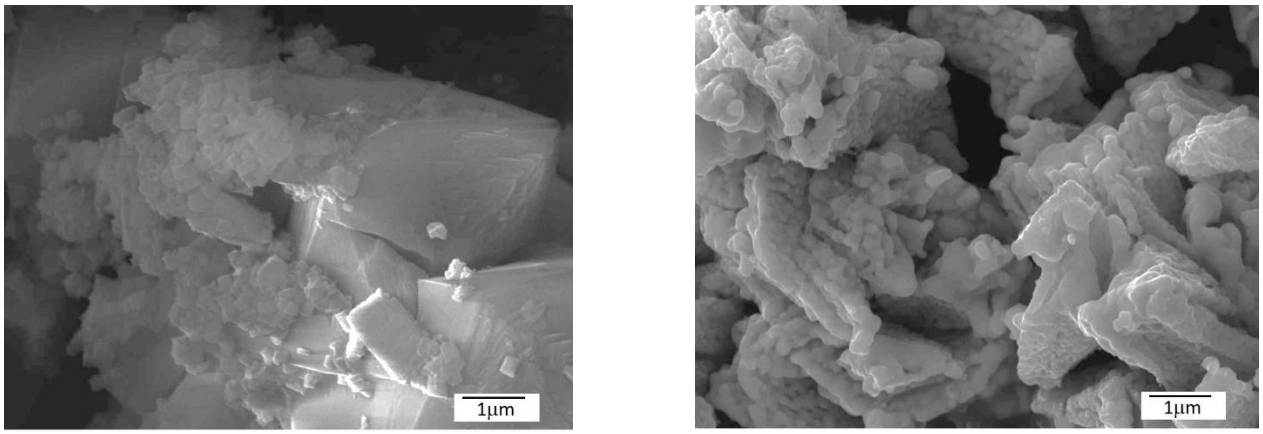

Figure 1 SEM images of morphological changes observed on sample ES 3: oxalate precursor as starting material (on the left); FeNi powder after thermal decomposition (on the right).

3.1 Characterization of thermal decomposition of ES3 precursor

Sample ES3 underwent thermal decomposition in a hydrogen atmosphere. The sample was heated to 600 °C and then cooled to room temperature. This process was conducted simultaneously in a laboratory furnace and in a vibrating-sample magnetometer equipped with the furnace, enabling the study of changes in the magnetic properties of the sample during annealing.

Microscopic observations of the sample after thermal decomposition revealed that the ratio of iron to nickel remained unchanged. The annealing time influenced the sample's morphology. Unlike to preceding study, where the sample formed a porous structure after being annealed at 320 °C for 20 hours in a hydrogen atmosphere [12], no such porous structure was observed in the ES3 sample. A comparison of the morphology of sample ES3 before and after thermal decomposition is presented in **Figure 1**.

The results of the magnetic measurements indicate that the decomposition of the precursor in H_2 begins at approximately 360 °C (**Figure 2**) and this first stage completes around 400 °C. Phase composition according to Mössbauer spectroscopy measurement at room temperature is as follows (in iron atomic fraction): 0.64 magnetite Fe_3O_4, 0.25 Fe-Ni alloy, and 0.11 remains of precursor. The spectrum is shown in **Figure 3**. The subspectra can be described by following hyperfine field parameters. Magnetite particles are represented with two sextets. The first one with hyperfine induction B_{hf} = 48.3±0.1 T, isomer shift IS = 0.31±0.01 mm/s, quadrupole shift QS_{sh}= 0.00±0.01 mm/s, and relative spectral area (equal approx. to atomic fraction of iron atoms) A_1=0.31±0.01. The second sextet has B_{hf} = 45.4±0.5 T, IS = 0.65±0.01 mm/s, QS_{sh}= 0.02±0.01 mm/s,

and A_2=0.33±0.01. Subspectrum ascribed to FeNi alloy particles are characterized by the sextet with B_{hf} = 28.3±0.1 T, IS = 0.04±0.02 mm/s, QS_{sh}=- 0.01±0.03 mm/s, and A=0.25±0.01. The third phase is represented by singlet with IS = 0.21±0.03 mm/s and A=0.10±0.01 and can be ascribed to precursor remains. The Mössbauer spectrum of the sample ES 3 after reduction in hydrogen atmosphere up to 600 °C was fitted using three subspectra which are ascribed to magnetite and FeNi particles. The first sextet of magnetite has B_{hf} = 48.8±0.6 T, IS = 0.11±0.07 mm/s, QS_{sh}= 0.10±0.09 mm/s, and A_1=0.22±0.02, the second one has B_{hf} = 45.8±0.5 T, IS = 0.53±0.05 mm/s, QS_{sh}= 0.02±0.01 mm/s, and A_2=0.31±0.01. The FeNi phase has subspectrum B_{hf} = 30.4±0.1 T, IS = 0.17±0.02 mm/s, QS_{sh}=- 0. 06±0.03 mm/s, and A=0.46±0.02. The phase composition and Mössbauer spectra parameters are in good agreement with previously published data. [6, 13, 14]. The change in the ratio of A_1/A_2 after annealing up to 600 °C in comparison with the annealing up to 400 °C very probably corresponds with oxygen stoichiometry in the magnetite.

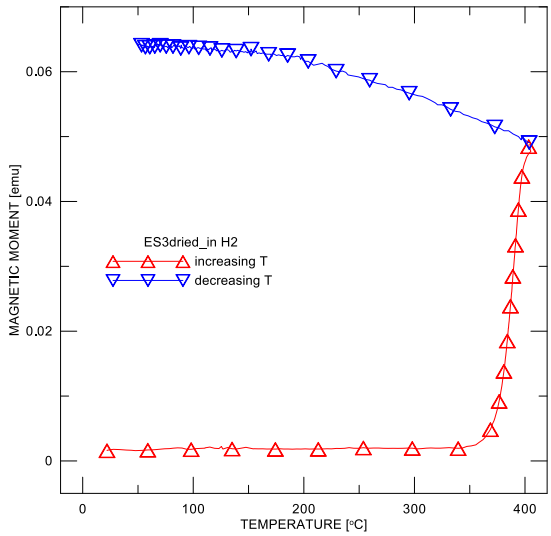

Figure 2 Magnetic measurement in H2 in field 50 Oe

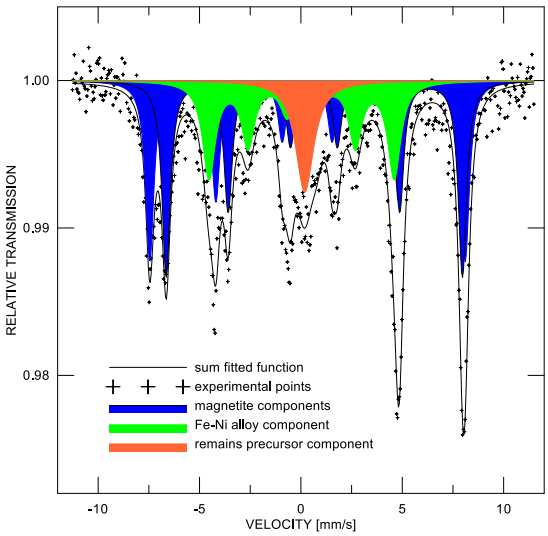

Figure 3 Mössbauer spectrum taken after magnetic measurement shown in Figure 2

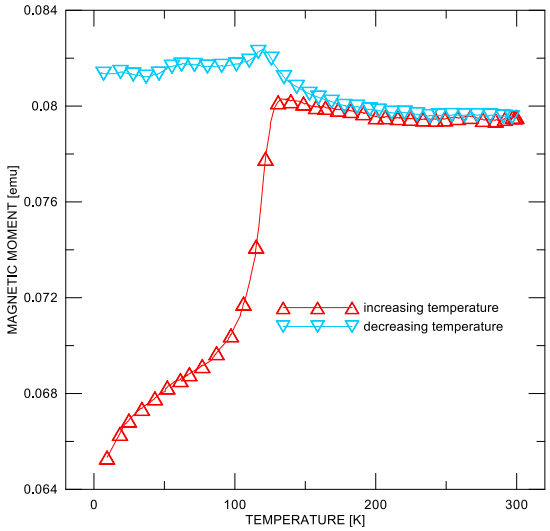

Figure 4 Temperature dependence of magnetic moment ZFC-FC of S3 sample after annealing in H2 at 600 °C.

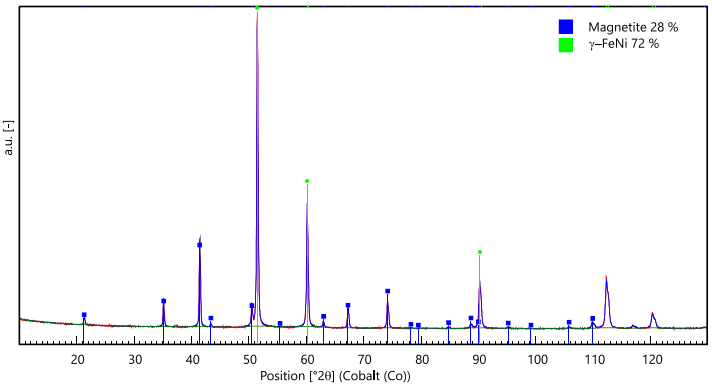

Figure 5 XRD of S3 sample after annealing in H_2 at 600 °C taken at room temperature.

Magnetic measurements of the ES3 precursor sample after annealing in H_2 up to 600 °C indicate a Curie temperature of 460 °C, which can be attributed to the Fe-Ni alloy component. Temperature dependence of magnetic moment ZFC-FC (Zero Field Cooled – Field Cooled) (**Figure 4**) confirms the presence of magnetite with the jumps at ~ 120 K (~ 150°C) corresponding to its Verwey transition.

The result of XRD (**Figure 5**) taken at room temperature confirms the magnetite and fcc FeNi phases in the ES3 sample after annealing in H_2 at 600 °C with mean coherent sizes 62 nm and 58 nm, respectively.

3. CONCLUSION

The morphology of $Fe_{(1-x)}Ni_xC_2O_4$ particles, studied through SEM, revealed a conglomerate of particles with diverse shapes, ranging from flakes to rectangular structures. EDS analysis confirmed a uniform distribution of iron and nickel, with the relative composition at 48% and 52% by weight, respectively. XRD identified the precursor as Iron Oxalate Dihydrate with an average particle size of 37 nm, while Mössbauer spectroscopy indicated the presence of Fe-Ni mixed-metal oxalates and iron sulphate monohydrate phases.

Characterization of the ES3 sample after thermal decomposition in a hydrogen atmosphere revealed the formation of magnetite and FeNi alloy particles. After annealing at 600°C, the mean crystallite sizes were determined to be 62 nm and 58 nm, respectively. These results suggest that the ES3 precursor is suitable for producing a mixture of magnetic nanoparticles with a Fe-Ni phase close to the desired $Fe_{50}Ni_{50}$ composition.

ACKNOWLEDGEMENTS

This work has been created by financial support and using of the research infrastructure of the Institute of Physics of Materials Czech Academy of Sciences, v. v. i.; CzechNanoLab project LM2023051 funded by MEYS CR is gratefully acknowledged for the financial support of the measurements at CEITEC Nano Research Infrastructure.

REFERENCES

[1] COEY, J.M.D. Pernament magnets: Plugging the gap. *Scripta Materialia.* 2012, vol. 67, pp. 524-529. https://doi.org/10.1016/j.scriptamat.2012.04.036

[2] CUI, J., KRAMER, M., ZHOU, L., LIU, F., GABAY, A., HADJIPANAYIS, G., BALASUBRAMANIAN, B., SELLMYER, D. Current progress and future challenges in rare-earth-free permanent Magnets. *Acta Materialia*. 2018, vol. 158, pp. 118-137. https://doi.org/10.1016/j.actamat.2018.07.049

[3] ABDU, Y.A., ERICSSON, T., ANNERSTEN, H. Coexisting antiferromagnetism and ferromagnetism in mechanically alloyed Fe-rich Fe–Ni alloys: implications regarding the Fe–Ni phase diagram below 400°C. *Journal of Magnetism and Magnetic Materials*. 2004, vol. 280, issue 1-2, pp. 395-403. https://doi.org/10.1016/j.jmmm.2004.03.036

[4] LEE, S., EDALATI, K., IWAOKA, H., HORITA, Z., OHTSUKI, T., OHKOCHI, T., KOTSUGI, M., KOJIMA, T., MIZUQUCHI, M., TAKANASHI, K. Formation of FeNi with L10-ordered structure using high-pressure torsion. *Philosophical Magazine Letters*. 2014, vol. 94, pp. 639–646. https://doi.org/10.1080/09500839.2014.955546

[5] YAO, Y., ZHANG, Ch., FAN, Y., ZHAN, J. Preparation and microwave absorbing property of porous FeNi powders. *Advanced Powder Technology*. 2016, vol. 27, issue 5, pp. 2285–2290. https://doi.org/10.1016/j.apt.2016.08.022

[6] ZHU, S., LI, N., ZHANG, D., YAN, T. Metal/oxide heterostructures derived from Prussian blue analogues for efficient photocatalytic CO2 hydrogenation to hydrocarbons. *Journal of CO2 Utilization*. 2022, vol. 64,102177 https://doi.org/10.1016/j.jcou.2022.102177

[7] DHANALAKSHMI, G., RAVICHANDRAN, V. Synthesis of nanocrystalline nickel-iron alloys-A novel chemical reduction method. *Chemical Physics Impact.* 2023. vol. 6,100202. https://doi.org/10.1016/j.chphi.2023.100202

[8] ŽÁK, T., JIRÁSKOVÁ, Y. Confit: Mössbauer spectra fitting program. Surface and Interface Analysis. 2006, vol. 38, pp. 710–714. https://doi.org/10.1002/sia.2285

[9] RAMANI, SATHYAVATHIAMMA, M. P., PUTTASWAMY, N. G., MALLYA R. M. Mössbauer Effect Study of the Thermal Decomposition in Hydrogen of Homogeneously Mixed Ferrous Nickel Oxalates with Different Iron to Nickel Ratios. *Physica Status Solidi (a).* 1983, vol. 77, issue 1, pp. 87–96. https://doi.org/10.1002/pssa.2210770110

[10] DEVILLERS, M., LADRIÈRE, J., APERS, D. Mössbauer study of 57Fe-doped simple and mixed dihydrated oxalates of bivalent metals (M = Mg, Mn, Fe, Co, Ni, Zn). *Inorganica Chimica Acta*.1987, vol.126, issue 1, pp. 71-77. https://doi.org/10.1016/S0020-1693(00)81242-6

[11] PETKOVA, V., PELOVSKI, Y., PANEVA, D., MITOV, I. Influence of gas media on the thermal decomposition of second valence iron sulphates. J*ournal of Thermal Analysis and Calorimetry*. 2011, vol. 105, pp. 793–803 https://doi.org/10.1007/s10973-010-1242-6

[12] ŠVÁBENSKÁ, E., ROUPCOVÁ, P., HAVLÍČEK, L., SCHNEEWEISS, O. Properties of nonocrystalline Fe-Ni particles prepared by thermal reduction of oxalate precursors. In: NANOCON 2023 Conference Proceedings 2023. Ostrava: TANGER Ltd., 2024, pp 76-82.

[13] LEHLOOH, A.F.D., MAHMOOD, S.H. Mössbauer Spectroscopy Study of Iron Nickel Alloys. *Hyperfine Interactions*. 2002, vol. 139, pp. 387–392. https://doi.org/10.1023/A:1021230926166

[14] VANDENBERGHE, R., BARRERO, C., DA COSTA, G., VAN SAN, E., DE GRAVE, E. Mössbauer characterization of iron oxides and (oxy)hydroxides: the present state of the art. *Hyperfine Interactions.* 2000. vol. 126, pp. 247–259. https://doi.org/10.1023/A:1012603603203